Engineering Science and Military Technologies
Volume (4) - Issue (1) - Mar 2020

ISSN: 2357- 0954
DOI: 10.21608/ejmtc.2020.34581.1147

Original Article

An integrated algorithm for structural health monitoring of composite plate using electromechanical impedance

Mostafa S. Amin and Mohamed A. M. Salem

Department of Civil Engineering, Egyptian Armed Forces, Military Technical College

Keywords:
Composite plates, electromechanical impedance, depolarization, finite element modeling, piezoelectric waver active sensor, self-diagnose , single Interrogation, structural health monitoring.

Corresponding Author:
Mostafa S. Amin, Department of Civil Engineering, Egyptian Armed Forces, Military Technical College, Cairo, Egypt, **Tel:** 01000368402, **Email:** melbeblawy@mtc.edu.eg

Abstract
The extra-ordinary development of structural materials, such as composite materials, and structural configurations necessitated establishing robust and continuous structural health monitoring (SHM) systems. The aim of the present work is to establish an integrated SHM algorithm to remotely detect damage starting from the insipient level for structures made of composite materials. It depends on the electromechanical impedance (EMI) technique using Piezoelectric Waver Active Sensor (PWAS). The algorithm procedure includes several subroutines developed to ensure the identification of real damage and relatively define its location and severity precisely. The performance and the reliability of the proposed algorithm are verified through numerical simulations carried out through finite element modeling of the monitored structure using ANSYS software, since it is available to do multi-physics modeling to simulate coupling characteristics of piezoelectricity. MATLAB codes are developed to prepare and process the obtained numerical data in order to implement the algorithm subroutines. Several numerical simulation studies are carried out to verify the proposed algorithm procedure and measure its performance. Carbon woven fiber composite plates equipped with a matrix of PWASs are assigned as test articles. Numerically, the algorithm was shown to be beneficial to detect two different-location of insipient damages and two different-location of insipient and moderate damages, as well as to locate these damages with accuracy more than 80%. Reliability of data obtained from physical operating system was guaranteed using sensors diagnostic check in advance to SHM process.

I. INTRODUCTION

The need of a sustainable monitoring system to guarantee the accepted integrity of structures arose a few decades ago. This system was denoted as structural health monitoring (SHM) system. Since then, many examples of working SHM systems were implied to detect and identify damages at early stage that cannot be detected using conventional means. Most reliable SHM systems depended upon modal analysis of structures, in other words, vibration-based damage identification (VBDI) SHM systems. For example, dynamic tests were conducted on Vasco da Gama Bridge, Portugal shortly before its opening in1998 by applying ambient and free vibration tests techniques using a set of forces balanced accelerometers[1]. Shimmizu Corporation 65-story 280-m tower, Singapore, was instrumented with monitoring system includes biaxial accelerometers erected in basement and roof levels in addition to a pair of anemometer to record wind and vibration response[2]. Among the SHM systems applied for a pre-stressed concrete bridge, a network of conventional strain gauges applied on Kishwaukee bridge, Illinois, the USA to provide health report via a real-time data acquisition and analysis[3]. Integrated and sustainable fatigue monitoring system was used in the European pressurized water reactor[4]. Amin[5] introduced a reliable health monitoring system for 8-bays aluminum space frame of span 5.65 meters used in simulating part of the international space station ISS structure, using a system of exciters, and response accelerometers. In his study, the response and excitation degrees of freedom are optimally selected to acquire minimum information of the modal data to be used in developing an integrated SHM algorithm. The algorithm was able to localize damage site and severity at single and multiple damage sites from light to sever damage levels.

Smart materials are designated materials that have one or more properties that significantly respond to external stimuli, such as stress and electric or magnetic fields.

One of the most common smart materials types with stunning capabilities is the piezoelectric ceramic. As stated earlier conventional SHM systems that employ

VBDI techniques depend mainly on studying the dynamic characteristics of the structure under surveillance via exerting suitable stimulation and record the response over the frequency range of interest, then frequency response function (FRF) spectrum is plotted[6]. The most similar approach for such a conventional monitoring concept is offered by piezoelectric waver active sensor (PWAS), which can be used to serve simultaneously as both sensor and actuator without having any non-stationary troubles during measurements. It is small patch that can be attached to the surface or embedded into the structural elements. This patch is capable of generating dynamic excitation force from hundreds of Hertz up to hundreds of KHz to avoid using heavy mechanical equipment.

The electromechanical impedance (EMI) technique is one of the techniques that benefits from PWAS advantages[7]. Electric (impedance/admittance) measured on the PWAS terminals can be considered as Frequency Response Function (FRF) for the host structure which is very similar to VBDI techniques. Comparing the resultant (impedance/admittance) spectra of pristine and defected cases for the host structure, valuable information about damage existence, severity and location can be interrogated. Also, the EMI technique has the advantage of having an easy post-sensing process compared to other VBDI techniques, in which the post-processing of measured applied dynamic excitation force and acquired velocity or acceleration data are needed.

Many successful attempts took place to establish SHM systems depending on EMI technique which proved to be such revolutionary solution for its ancestral VBDI technique problems, especially huge size and weight of used equipment compared to innovative sensors that can be easily attached or integrated in the structures permanently. Gulizzi *et al.*[8] proposed SHM algorithm depend on the simultaneous usage of EMI and guided wave exerted by PZT patches. Medeiros *et al.*[9] developed hybrid SHM system to identify damage in composite plates. This system implies PZT transducer to detect the existence of damage as well as global localization, optical method (shearography speckles) test was performed then to localize the damage. Hoshyarmanesh *et al.*[10] established an EMI low-cost, small-size portable transceiver circuit to detect flaws in moving/rotary structures. Samantaray *et al.*[11] conducted laboratory investigation to detect bolt looseness of prototype structure using single PZT patch.

In the current work, a novel algorithm is proposed aiming to establish a reliable SHM system depends on EMI technique and able to carry out surveillance of structures made of epoxy carbon fiber composite plate through 4 main stages using a matrix of attached PWASs:

a) Establish a pristine spectrum set of the monitored structure.

b) Carry out a global check for the existence of flaws using a single operation.

c) Perform panel by panel check in case of recording global damage to quantify the damage.

d) Finally, carry out a local investigation in the panel of the damage to localize damage.

The above processes are carried out by manipulating parallel and single data interrogation techniques for the same PWASs matrix. The proposed algorithm depends on acquiring data over different frequency ranges to benefit from any possible changes in the modal data due to damage. Self-diagnose check is integrated into the algorithm to sustain the reliability of interrogated information.

II. PROPOSED ALGORITHM PROCEDURE

MATLAB codes are developed to manipulate acquired data and implement the sequential procedures of algorithm's sub-routines. Figure 1 illustrates the flow chart of the proposed algorithm. In order to verify the proposed algorithm performance, 530 × 250 ×3 mm composite plate is assigned as a test article. The plate was equipped with eight PWASs that formed three panels (panel (1,1), panel (1,2), and panel (1,3)) as shown in Figure 2. The algorithm procedure sequence can be summarized as follows:

Phase (I): In pristine case (denoted by blue polygonal)

- Parallel interrogation is carried out using PWASs placed at the corners of the composite plate (panels (1,1), (1,4) , (2,1) and (2,4)) to acquire real part of EMI over low frequency range (first 5 natural modes). The calculations are performed and stored based on equations 5 to 7 that will be illustrated later.

- Numbers of desired sub-panels rows and sub-panels columns (which are denoted as Rm and Tn respectively) are set by operator (they are set here to be 1and 3, respectively). Parallel interrogation is carried on each panel separately at high frequency range (which is set here to 570-700 KHz).

- Single interrogation over high frequency is carried out for all PWASs from panels (1, 1) to (2,4) at high frequency range.

- The aforementioned procedures are carried out to file all the EMI spectrums for the healthy plate and to be used as a baseline data for root mean square deviation RMSD and damage detection index DDI calculations.

- Proposed algorithm carries out general periodic parallel interrogation (PWASs (1,1), (1,4), (2,1) and (2,4)) at low frequency range (405- 1065 Hz). If the damage occurs to the monitored composite plate, RMSD and/or DDI indices record a non-zero value greater than the assigned threshold, which indicates the presence of damage.

Phase (II): In damage case (denoted by red polygonal)

- Self-diagnose sub routine, Figure 3, is carried out to make sure that recorded index, RMSD or DDI, is not due to a false prediction (PWAS malfunction). In case that the RMSD or DDI values found to be greater than the assigned threshold, this means that there is a presence of damage.

- Parallel interrogation is carried out separately for each panel of the preset number of panels, at high frequency, to identify the panel that is affected by damage.

- If one or more panel record value of RMSD or

DDI indices greater than the preset threshold, single interrogation is performed to the four PWASs which are forming the recorded panel at its corners.

- Self-diagnose subroutine is performed again to avoid any miss data due to PWAS malfunction.
- Finally, the center of mass principle, that will be explained later and represented by equations 10 and 11, is implemented to estimate probable damage locations.

In the following subsections, the algorithm main subroutines are explained.

II.1 SELF - DIAGNOSE

The integrity and reliability of the hardware parts of the SHM system should be maintained to avoid incompetence that occurred due to a failure of SHM proposed system components. This step is crucial to grantee the efficiency and creditability of periodic SHM process. There are two possible sources for system false prediction, probable malfunction of the PWAS itself and de-lamination between the host monitored structure and PWAS. Figure 3 illustrates self-diagnose check subroutine for the hardware components (PWASs). It is considered as a major component of the proposed algorithm and carried out using EMI technique. The implementation of the subroutine is carried out through numerical simulation using ANSYS finite element package to investigate the impact of PWAS desponding and possible PWAS malfunction on the imaginary part of admittance spectrum.

$$\begin{bmatrix}\{T\}\\ \{D\}\end{bmatrix} = \begin{bmatrix}[c^E] & -[e]^T\\ [e] & [\varepsilon^S]\end{bmatrix}\begin{bmatrix}\{S\}\\ \{E\}\end{bmatrix} \quad (1)$$

$$\begin{bmatrix}\{S\}\\ \{D\}\end{bmatrix} = \begin{bmatrix}[s^E] & -[d]^T\\ [d] & [\varepsilon^T]\end{bmatrix}\begin{bmatrix}\{T\}\\ \{E\}\end{bmatrix} \quad (2)$$

where:
{S} : Vector of stress
{T} : Vector of strain
{D} : Electric charge vector
$[C^E]$: Fixed field stiffness matrix of the piezoelectric material
$[S^E]$: Fixed field compliance matrix of the piezoelectric material
[e] : Piezoelectric constant matrix for stress-charge formula
[d] : Piezoelectric constant matrix for strain-charge formula
$[\varepsilon^S]$ and $[\varepsilon^T]$: Permittivity matrices at fixed strain & at fixed stress respectively.
{E}: Electric field

II.2. SINGLE AND PARALLEL INTERROGATION

Tzou H.S. and Tesng C.I.[12] introduced the expression for the coupling between mechanical actions and electrical variables response that are exhibited by piezoelectric materials. IEEE standard[13] and Ikeda[14] generalized the plane formula introduced by Tzou and Tesng into well-known 3D piezoelectric constitutive equations 1 and 2. These equations have been used by Liang *et al.*[15] to drive mathematical formula equation 3 for the admittance (inverse of the impedance) at the terminals of simple 1-D model that describes PWAS attached to mass spring system shown in Figure 4.

Zagrai[16] introduced mathematical model that describes 2-D limited geometrical configuration models. A hybrid analytical-numerical model was introduced by Bhalla[17] to identify the mechanical impedance of any monitored structure regardless its material or shape formula using the advance of finite element (FE) software package. Gresil *et al.*[18] and Salem[19] introduced verified fully numerical simulation for acquiring EMI at PWAS terminals attached to composite plates with different scenarios of damage.

In order to acquire the EMI spectrum of the structural system under surveillance using finite element modeling, the attached PWAS is stimulated with a load of 1 volt over designated frequency range. Then, complex current $\bar{I}$ is calculated using equation 5.

$$Y(\omega) = j\omega \frac{w_a l_a}{t_a}\left(\hat{\varepsilon}_{33}^T - d_{31}{}^2\hat{Y}_p^E + \frac{Za(\omega)}{Za(\omega)+Zs(\omega)} \times d_{31}{}^2\hat{Y}_p^E\left(\frac{\tan kl_a}{kl_a}\right)\right) \quad (3)$$

where:

$$Z(\omega) = 1/Y(\omega) \quad (4)$$

And
Y(ω) : Electric admittance at PWAS terminals
j : Imaginary component
ω : Angular velocity
w_a l_a t_a : PWAS dimensions (width, length and thickness)
$\hat{\varepsilon}_{33}^T$: Complex permittivity in z direction
d_{31} : Piezoelectric constant component (strain-charge formula)
$\hat{Y}_P^E$: Complex young modulus of PWAS at constant field
Za (ω) : Mechanical impedance of PWAS
Zs (ω) : Mechanical impedance of host structure
K : Wave number

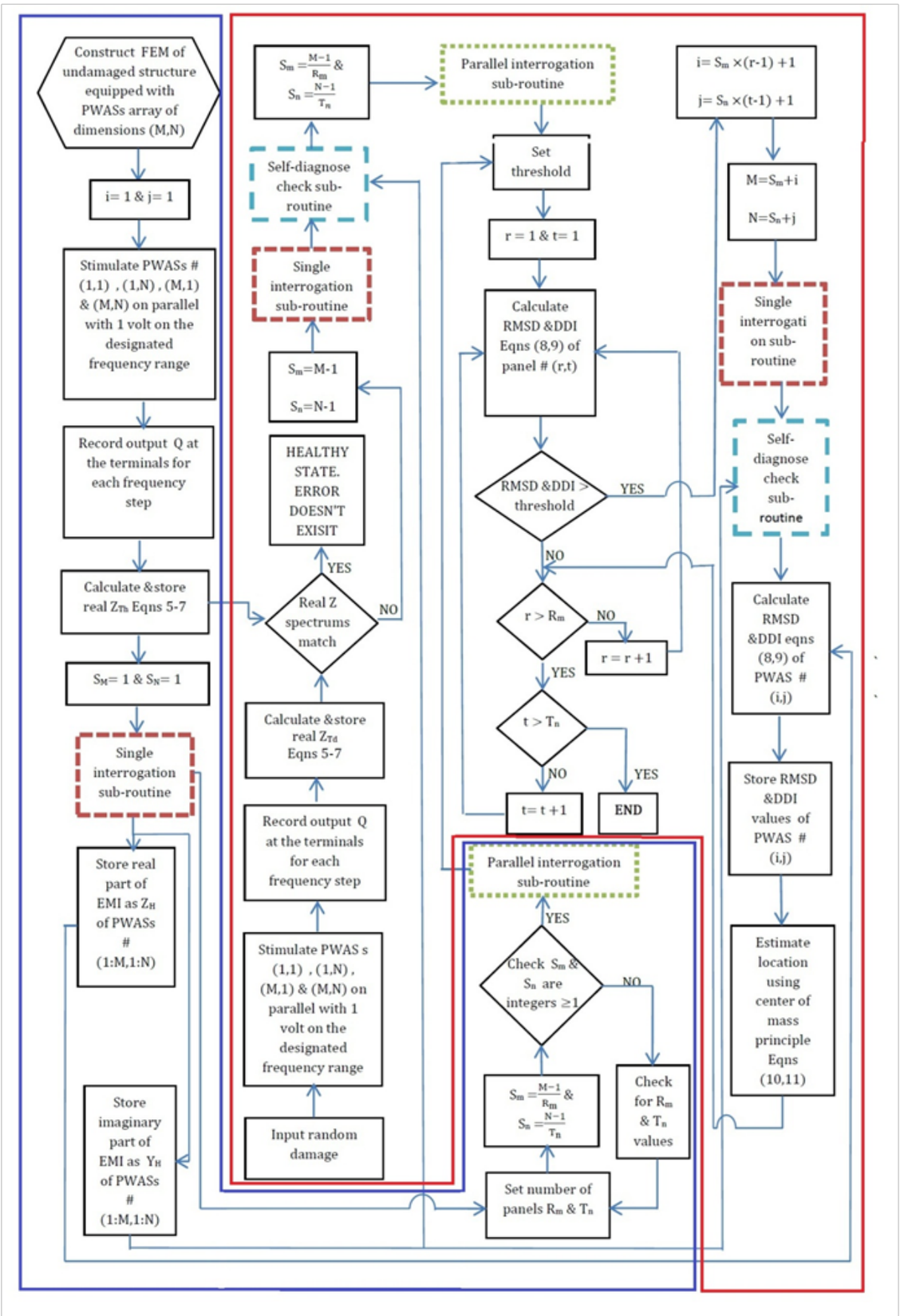

Fig. 1: Proposed SHM algorithm.

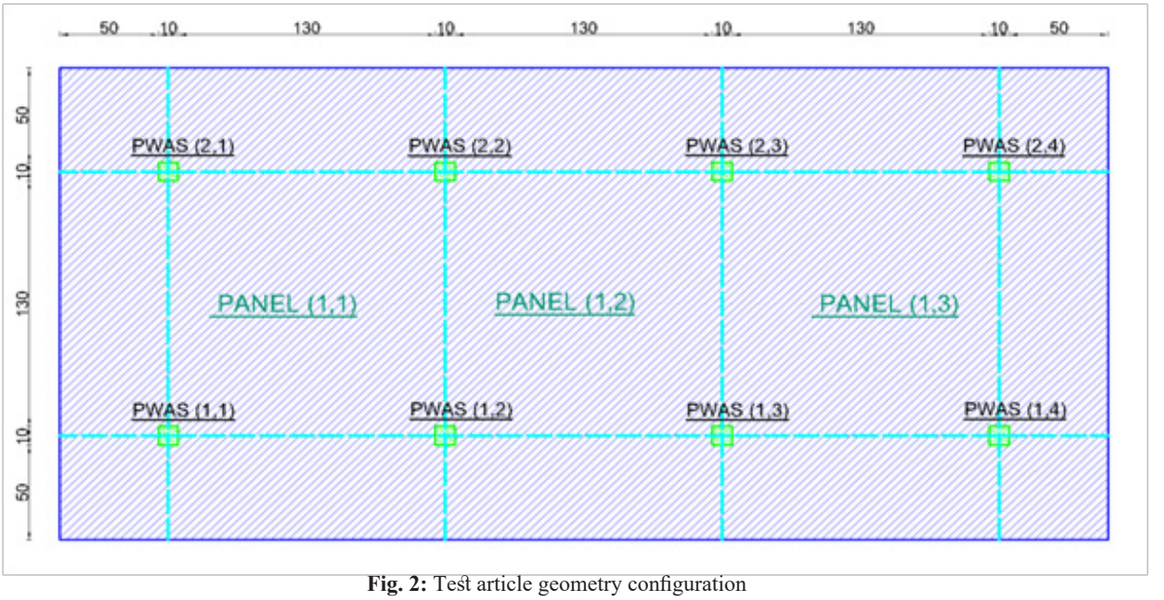

Fig. 2: Test article geometry configuration

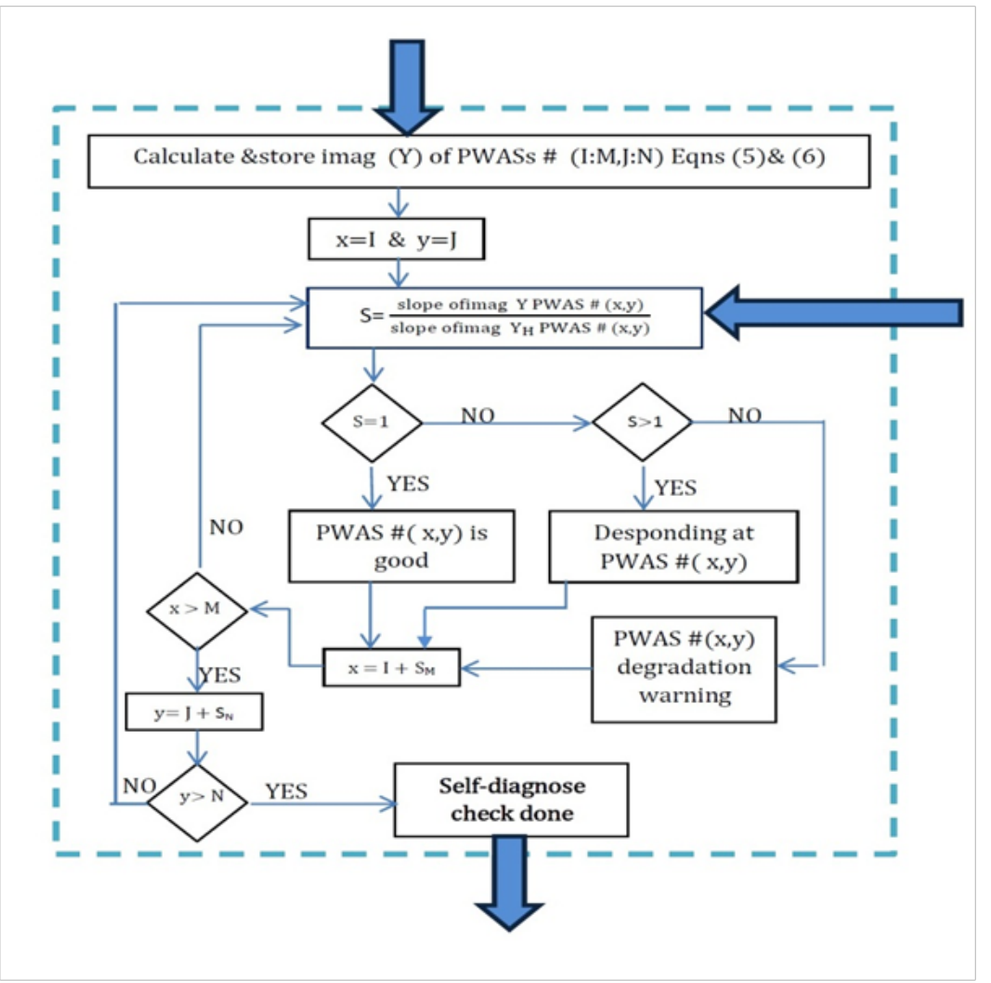

Fig. 3: Self-diagnose check sub- routine.

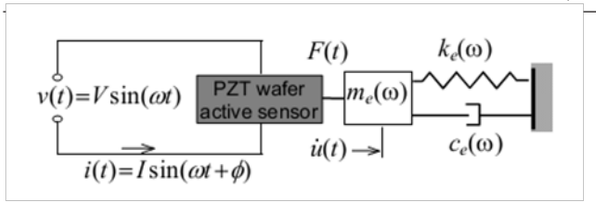

Fig. 4: Electro-mechanical coupling between PZT patch and structure introduced by Liang *et al.*[15].

$$\bar{I} = i\,\omega \sum Q_i \qquad (5)$$

Where: $\sum Q_i$ is the summation of nodal charges that obtained at PWAS terminals from numerical simulation. EMI is calculated using equations (6) and (7) knowing input voltage (assigned as 1 volt in the current study).

$$\bar{Y} = \bar{I}/\bar{V} \qquad (6)$$

$$\bar{Z}(\omega) = 1/\bar{Y} \qquad (7)$$

Single interrogation technique is the process where the PWASs are stimulated individually to acquire several interrogated EMI spectra.

Parallel interrogation technique is the process where the PWASs are connected in parallel as the stimulation and interrogation process are carried out simultaneously through two general terminals resulting in one general EMI spectrum[20, 21]. Figure (5) illustrates the difference between setting-up (n) PWASs for the two interrogation system.

The proposed algorithm includes both techniques applied for a matrix of (M) rows and (N) columns attached to the composite plates. Figure (6) illustrates the sub-routine flow chart developed for single interrogation technique implementation, in which simple loop is followed, as each PWAS (i,j) is stimulated and the output Q is recorded at the terminals over the desired frequency range. Figure (7) illustrates parallel interrogation sub-routine where (R_m) is designated a number of panels' rows and (T_n) is the designated number of panels' columns.

Hey *et al.*[21] introduced several algorithms to carry out parallel interrogation, such as doing it row by row or panel by panel. To achieve such manipulation in the proposed algorithm (R_m) and (T_n) are entered by the user to determine the size of the desired parallel interrogation panel.

(a)

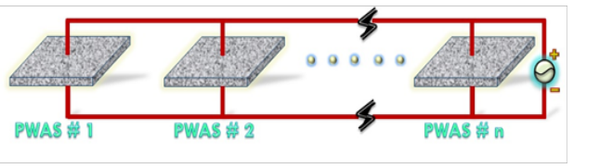

(b)

Fig. 5: (a) single interrogation set up (b) parallel interrogation set up.

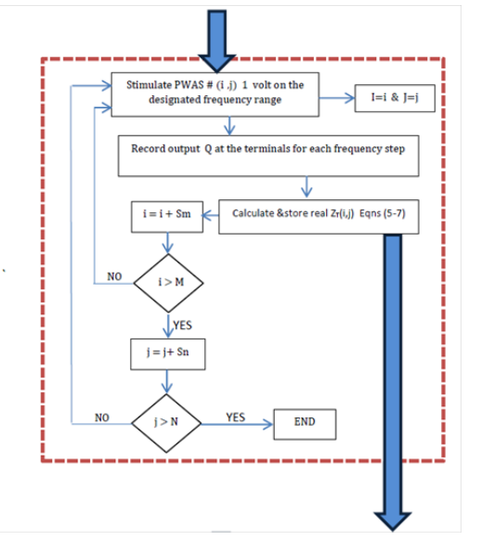

Fig. 6: Single interrogation sub-routine

II.1. MATHEMATICAL IDENTIFICATION INDICES

The EMI technique unlike classic SHM vibration based techniques - it can capture any changes in the pristine spectrum due to any damage level. The discrepancy between healthy and defected spectrums reveals information about damage existence and severity. The comparison between both spectrums is carried out through the implementation of damage indices on the impedance raw data.

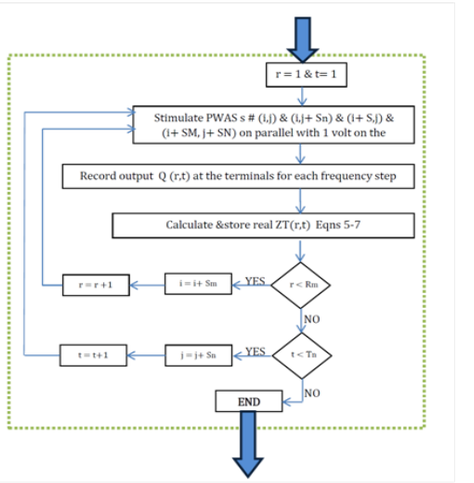

Fig.7: Parallel interrogation sub-routine.

The damage index is a scalar quantity produced from the processing of two spectra (pristine and damaged) and reveals the difference between them. Its value serves as an indicator for the damage existence in the structure. Two statistical indices are implemented herein, root mean square deviation (RMSD)[17,18] represented by mathematical formula (8), and Damage Detection Index (DDI) which introduced by Napolitano *et al.*[23] and modified by Amin *et al.*[24] and represented by mathematical formula (9). The RMSD found to exhibit relatively higher values other than the values calculated by the modified DDI which enabled the ability to reveal the occurrence of any incipient damage Salem[19].

$$\text{RMSD}\,\% = \sqrt{\frac{\sum[\text{Re}(Z_i)-\text{Re}(Z_i^0)]^2}{\sum[\text{Re}(Z_i^0)]^2}} \times 100 \qquad (8)$$

$$\text{DDI}\,\% = \left(\frac{\sum|FI_i - FD_i|}{\sum FI_i}\right) \times 100 \qquad (9)$$

where :

Z_i^0 : The recorded impedance of PWAS at pristine state of order (i)

Z_i : The recorded impedance of PWAS at defected condition of order (i)

FI_i : Amplitude of frequency response functions of healthy structure of order (i)

FD_i : Amplitude of frequency response functions of damaged structure of order (i)

The damage location is linearly proportional to the nearest PWASs, which is simply helpful to localize damage by applying the center of mass principle with statistical RMSD indices which utilized by Saafi and Sayyah[25], which mathematically expressed by equations 10 and 11.

$$\bar{X} = \frac{\sum_{i=1}^{n}(RMSD_i x_i)}{\sum_{i=1}^{n}(RMSD_i)} \qquad (10)$$

$$\bar{Y} = \frac{\sum_{i=1}^{n}(RMSD_i y_i)}{\sum_{i=1}^{n}(RMSD_i)} \qquad (11)$$

where; $\bar{X}$ and $\bar{Y}$ are the coordinates of damage location, x_i and y_i are the coordinates of i^{th} PWAS, and n is the number of used PWASs

This can be attributed to the high frequency effect that brought vibrations to be concentrated in the vicinity of PWASs, hence, the closer PWASs were more sensitive to the occurrence of such incipient damage[26].

II.2. FREQUENCY RANGES

Among the significant differences between VBDI and EMI SHM techniques is the operative frequency range. The most sensitive damage indices are introduced in the frequency ranges of the higher peaks density, Zagrai[16]. In the current study, the spectrum shown in Figure 8 is typical EMI spectrum interrogated in single manner, as it is divided into three frequency ranges aiming to satisfy certain characteristics as follows:-

- The first frequency range from (570 to 2150 Hz.); this range includes the first lower modes that have a significant contribution to the total strain energy, which has a remarkable influence in the damage detection as concluded by Amin[5].
- The second frequency range from (10 to 100 KHz.); this region satisfies the characteristics stated byZagrai[16].
- The third frequency range from (150 to 300 KHz.); this region is assigned to examine the performance of EMI at high frequency range.

II.4. FINITE ELEMENT MODELING

In order to implement the proposed novel algorithm procedure, the numerical simulation procedure includes finite element modeling of the assigned test article that is constructed commercial package, ANSYS version 15.0[29]. The elements types used to model both PWAS and composite plates are selected from ANSYS library.

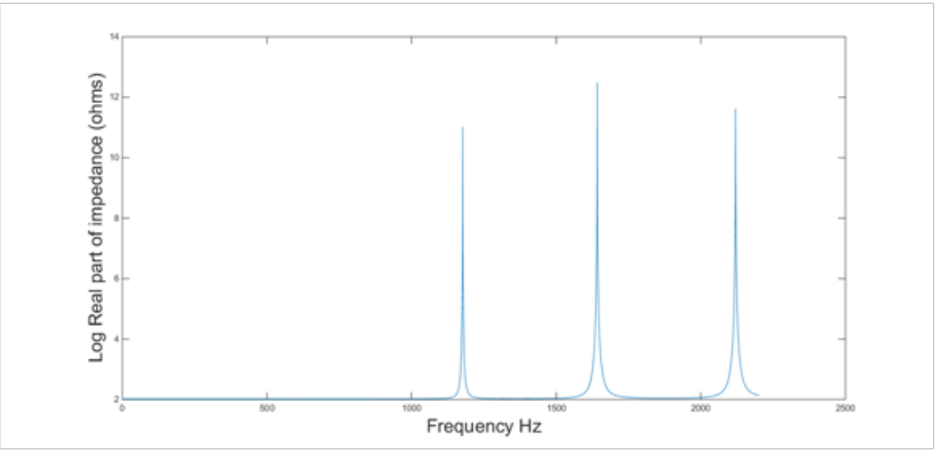

(a) Frequency range: (0-2150 Hz)

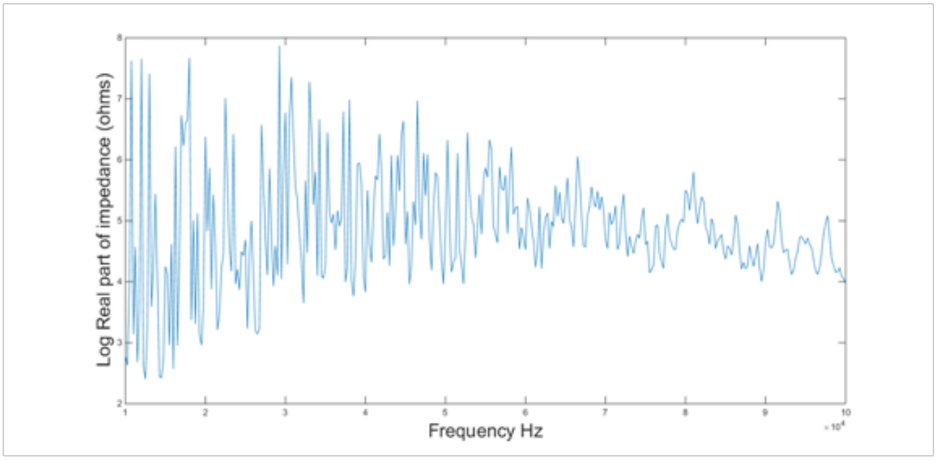

(b) Frequency range: (10-100 KHz)

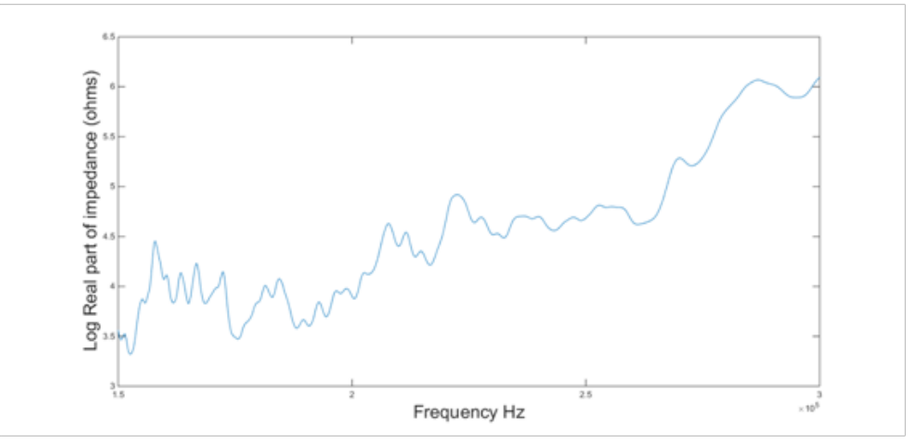

(c) Frequency range: (150- 300 KHz)

Fig. 8: Real part of EMI spectrum from (0-300 KHz).

II.5. FINITE ELEMENT MODELING

In order to implement the proposed novel algorithm procedure, the numerical simulation procedure includes finite element modeling of the assigned test article that is constructed commercial package, ANSYS version 15.0[29]. The elements types used to model both PWAS and composite plates are selected from ANSYS library.

- Finite element modeling for PAWS

The PWAS patch assigned for the current research is 10×10×0.5 mm attached to the monitored composite plate. It is made of APC850 material has the properties illustrated in Table (1), matching the American Piezoelectric Ceramics APC850. The (SOLID226) cubic coupled element is selected to model the PAWS. It has eight nodes each of which has 6 DOFs (thermal, magnetic, and electric DOFs in addition to translations in the nodal x, y, and z directions), only four of them are assigned for the current study, which are translations in the nodal x, y, and z directions in addition to electric DOFs.

- Finite element modeling for test article

The test articles assigned for verifying the algorithm procedures are 530×250×3 mm plates made of six layers of pre-defined material in ANSYS library software which is denoted as Epoxy_Carbon_Woven_395GPa_ Preprege $[0]_s$[29] with mechanical properties shown in Table (2). The (SHELL181) element is selected to model the composite plate. The element has eight nodes each of which has six DOFs (translations in the nodal x, y, and z directions and three rotations around the same directions). The plate is monitored using eight PAWS's at the corners of three panels as shown in Figure (2).

III. NUMERICAL SIMULATION FOR PROPOSED ALGORITHM VERIFICATION

- Self-Diagnose of PWASs

The implementation of self-diagnoses sub-routine illustrated in Figure (3) for PWASs is carried out through numerical simulation using finite element modeling .The size of element (SOLID226) which is used to simulate PWAS, was denoted to be 1.4 mm, while the size of (SHELL281) which is used to simulate the test article denoted to be 2.5 mm to achieve considerable convergence using frequency upper operating limit (1065 Hz). The boundary conditions of the test article were set to be fixed-fixed. The simulations carried out using the EMI technique as it considered the possible malfunction of the PWASs due to desponding of the adhesive layer and / or due to the PWAS depolarization.

Table 1: Material properties of APC850

Physical Property	Value
E_1,E_2	63.24 GPa
E_3	54.00 GPa
G_{13},G_{23}	22.00 GPa
G_{12}	24.00 GPa
ν_{13} , ν_{23}	0.41
ν_{12}	0.3
ρ	7600 kg/cm^3
ε^s_{11}	0.968e-8 F/m
ε^s_{33}	0.668e-8 F/m
e_{31}	-8.02 C/m^2
e_{33}	18.31 C/ m^2
e_{15}	12.84 C/ m^2

- Desponding of Adhesive Layer

A parametric study is carried out Amin and Salem[28] to investigate the impact of propagation of desponding between PWAS and the monitored composite plate on the imaginary part of admittance spectrum. The simulation studies considered different levels of area desponding between PWAS and host structure (0%, 36%, 64%, 84% and 100%). The simulation results show that remarkable up shifting in the base line of imaginary admittance spectrum occurs and slope angle of the spectrum increases with the increase of the area desponding percentage, as shown in Figure (9). This result matches with experimental results obtained by Park *et al.*[7] regarding the same issue. Accordingly, this step is crucial in the proposed algorithm as the base-line of the imaginary admittance spectrum is acquired for the healthy case and used as a reference for self-diagnose check.

Table 2: Material properties of Epoxy_Carbon_Woven_395GPa_ Preprege.

Properties	Epoxy_Carbon_Woven_395GPa_Preprege
E_1, E_2	91.82 GPa
E_3	9.00 GPa
G_{13},G_{23}	3.00 GPa
G_{12}	19.5 GPa
ν_{13}, ν_{23}	0.3
ν_{12}	0.05
ρ	1480 kg/cm^3

where :
E_1,E_2 ,E_3 : Young's moduli for directions x,y, and z
G_{13},G_{12},G_{23} : Modulus of shear rigidity
ν : Poisson ratio
ρ : Density

PWAS Malfunction due to Mass Loss or Depolarization

PWAS malfunction can be caused either by the degradation of PWAS coupling properties (depolarization) that may happen due to life time or operational conditions or due to partial loss of mass of the PWAS due to hard impact. The simulation results carried out by Amin and Salem[28] for simulated PAWS malfunction for mass loss and depolarization show downward shift in the imaginary part of the admittance Y(ω) as shown in Figure (10) and Figure (11), respectively. These results coincide with the conclusions reached by Park *et al.*[27].

Based on the results of these numerical simulations, it is proved that there is a possibility of having falls detection of damage due to the influence of PWAS adhesive layer desponding or PWAS malfunction. Consequently, self-diagnose of the PAWSs is considered as a curial step of the proposed algorithm.

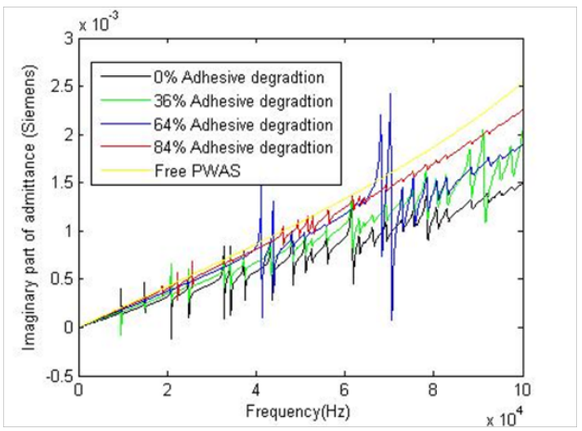

Fig. 9: Relation between frequency and imaginary part of admittance in case of desponding propagation by Amin and Salem[28].

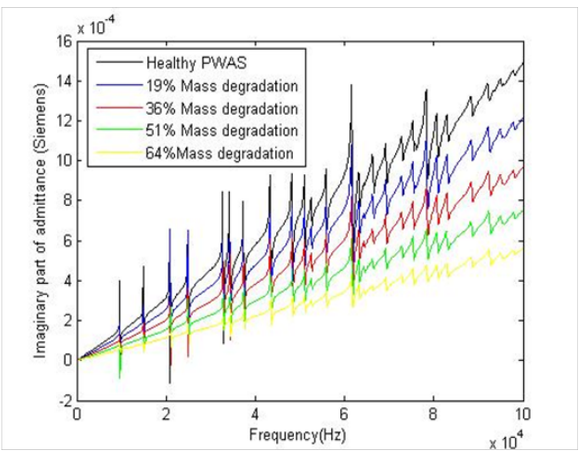

Fig. 10: Relation between frequency and imaginary part of admittance in case of mass loss cases by Amin and Salem[28].

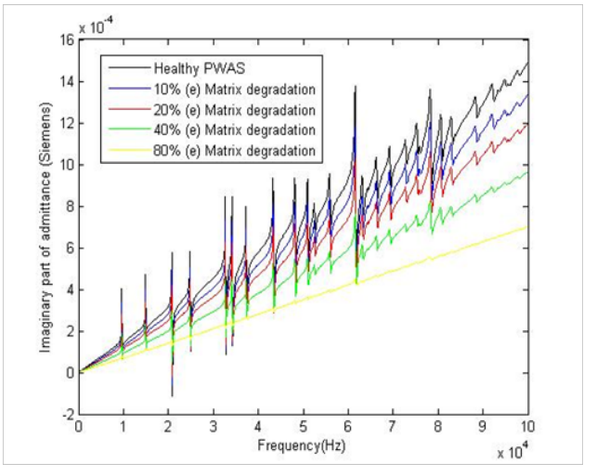

Fig. 11: Relation betweenfrequency and imaginary part of admittance in case of piezoelectric depolarization.

Damage Identification Cases

Single site damage cases

Salem *et al.*[30] carried out a parametric study through numerical simulation on 250×250×3 mm composite plate of the same material described in Table (2) equipped with four PWASs of the same material described in Table (1). This study was a part of the current research in which single site simulated damage scenarios were carried out to test the ability of part of the proposed algorithm in identifying damage. Only the damage indices (RMSD and modified DDI) were applied for identification. The damage simulation included three levels (sever, medium and light). The calculated damage indices values are representative of damage severity and can be used to relate the distance between PAWS and damage location

Multiple sites damage cases

To measure the performance of the proposed integrated algorithm in identifying damage at multiple sites, numerical simulation studies are carried out on the assigned test article (530 × 250 ×3 mm composite plate equipped with eight PWASs) shown in Figure (2). Two damage scenarios are introduced at two predefined locations with different severities as shown in Figure (12) and Figure (13).

Damage Case 1: Two locations are damaged in panels (1,1) and (1,3) as shown in Figure (12), each of which dimension is 10×10 mm as the stiffness of the first layer is reduced by 95%. Both simulated damage locations are considered as incipient damages.

Damage Case 2: Two locations are damaged in panels (1,1) and (1,3) as shown in Figure (13), the first location at panel (1,1) has an area equal to 10×10 mm and the second location at panel (1,3) has an area of 30 ×30 mm as the stiffness of the first four layers for both locations are reduced by 95%. The first simulated damage location at panel (1,1) is considered as incipient damage, while the second simulated damage location at panel (1,3) is considered as moderate damage.

Damage Identification Procedure

The procedure described earlier are implemented herein as the proposed algorithm carries out general periodic parallel interrogation for PWASs (1,1), (1,4) , (2,1) and (2,4) at low frequency range (405-1065 Hz) to make sure that RMSD and DDI recorded values not greater than the preset threshold.

If RMSD and DDI values are recorded, self-diagnose sub routine is carried out to make sure that recorded indices are due to real damage and is not falls prediction due to PWAS malfunction Figure (3).

According to preset number of panels, parallel interrogation is carried out separately for each panel at high frequency to find out which panel has the damage. If one or more panel record value of RMSD index over than preset threshold, single interrogation is carried out to the four PWASs which are forming the recorded panel.

Self-diagnose subroutine is carried out to avoid any miss data due to PWAS malfunction.

Single interrogation is carried out for the PWASs of damaged panel and the RMSD indices are calculated for each.

Finally, the raw data acquired in the previous step is used to precisely identify damage location by implementing the center of mass principle represented by equations (10, 11).

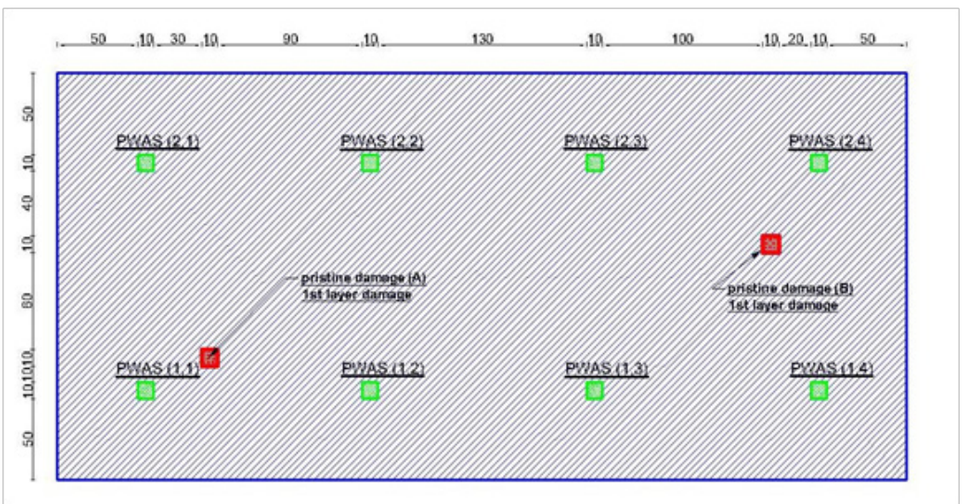

(a) Geometry

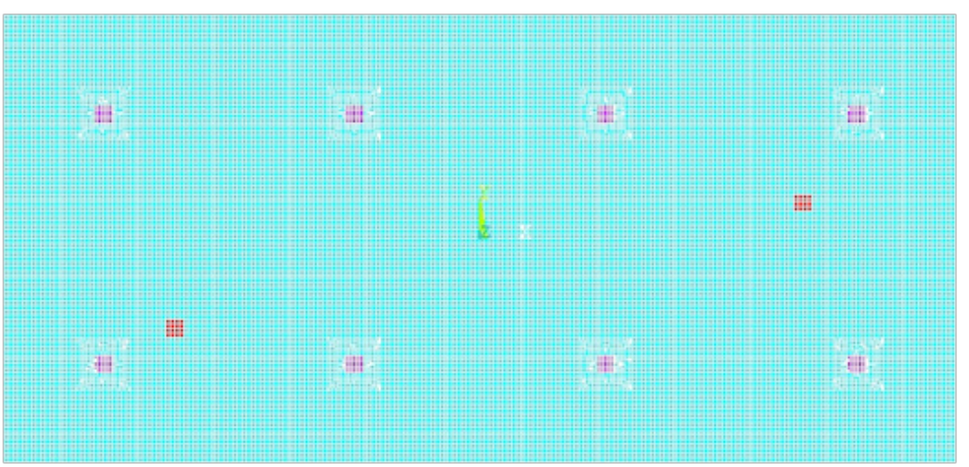

(b) Finite element model

Fig. 12: Location of simulated damage Case (1).

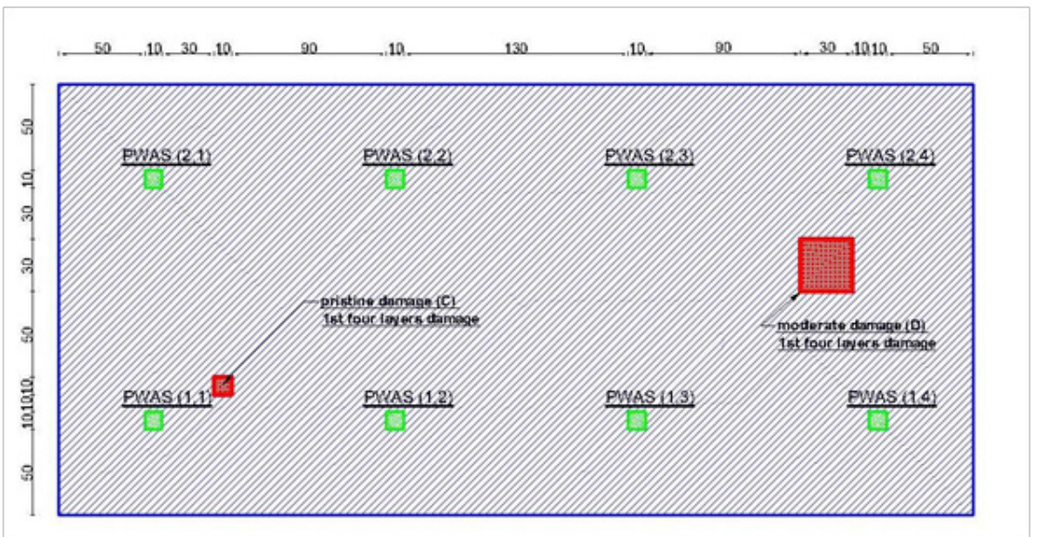

(a) Geometry

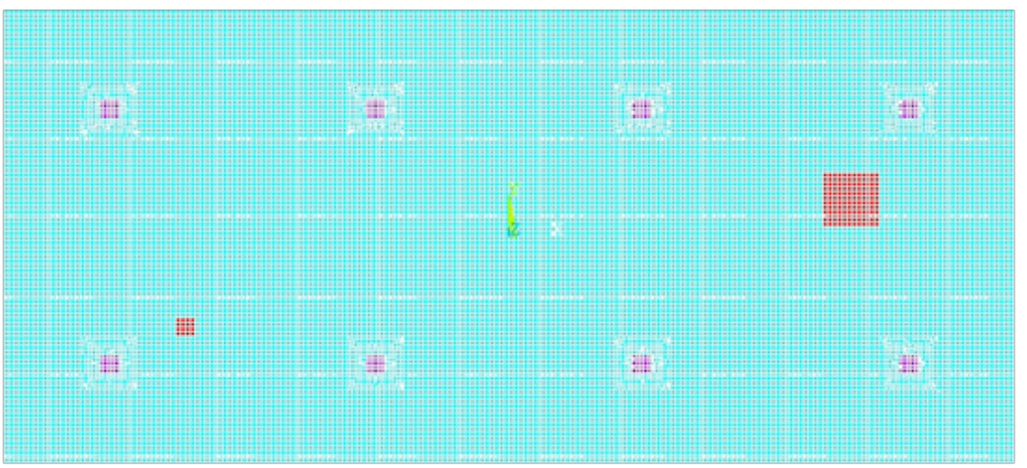

(b) Finite element model

Fig. 13: Location of simulated damage Case (2).

III.3. RESULTS AND DISCUSSION

For both damage cases the implementation of self-diagnoses subroutine leads to the conclusion that the recorded RMSD indices are above the expected values that may be created by PAWS malfunctioning.

Consequently, implementation of parallel interrogation subroutine over the lower frequency range for PWASs (1,1), (1,4) , (2,1) and (2,4) revealed the occurrence of the damage since the recorded RMSD's are relatively high with values 101.3% and 150.8% for damage cases (1) and (2) respectively.

Figure (14) illustrates the recorded RMSD values for panels (1,1), (1,2) and (1,3) acquired from parallel interrogation of each panel at high frequency range. These values are well representative for damage existence in both panels in addition to the severity of each case of damage.

In order to identify the damage locations, a single interrogation subroutine is performed for PWAS's surrounding panels (1,1) and (1,3) over the high frequency range. Figure (15) illustrates the RMSD values that are related to the relevant PAWS's. The nearest PWAS becomes sensitive to damage than the others and these values are used through the implementation of the center of mass principle to the data acquired in this stage, which is listed in Table (3). The results of this step are listed in Table (4), where damage location in each panel for each damage case is identified with relatively acceptable precession.

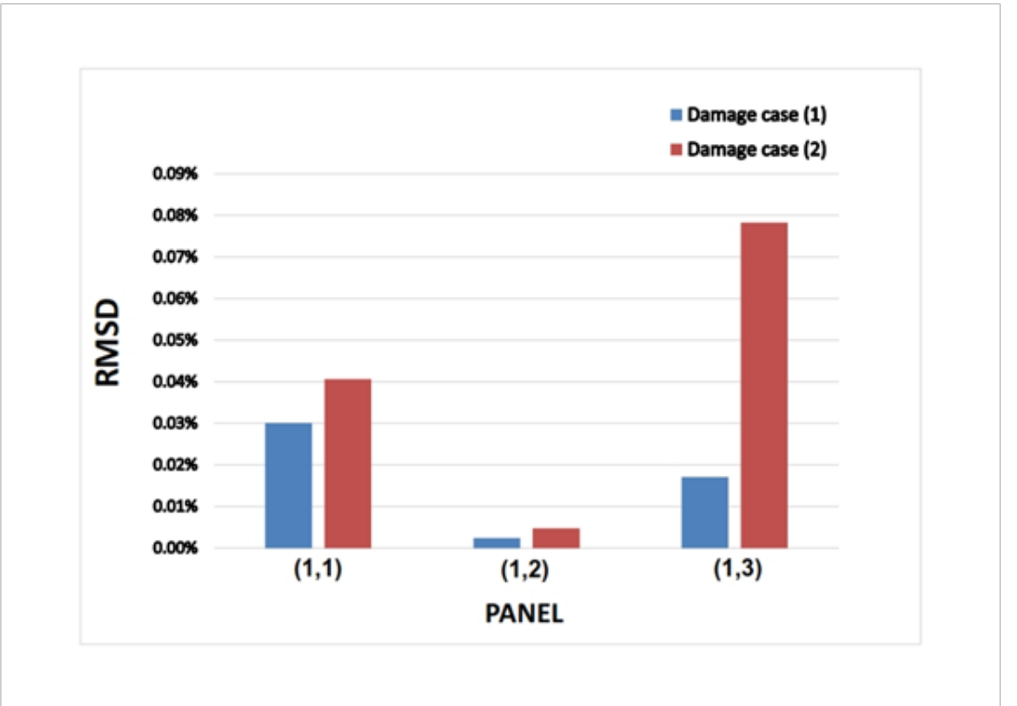

Fig. 14: RMSD resulted from parallel interrogation process of each panel over frequency range (570-700 KHz.).

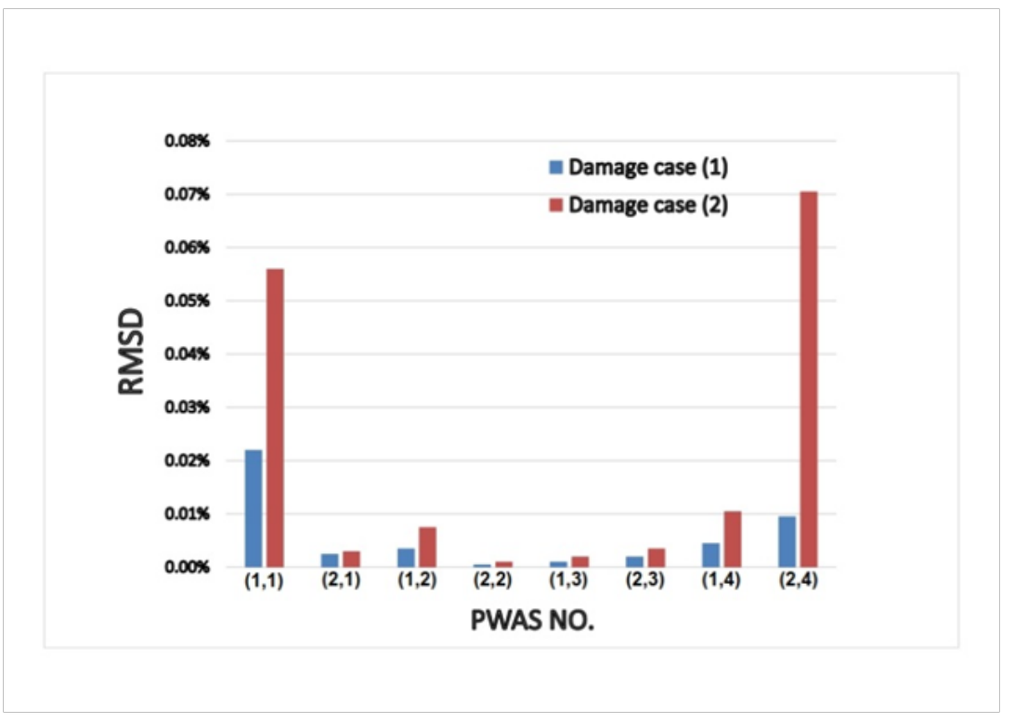

Fig. 15: Values of RMSD due to single interrogation over frequency range (570-700 KHz.).

Table 3: Values of RMSD resulted from single interrogation process.

PWAS NO.	RMSD % Case (1)	RMSD % Case (2)
(1,1)	0.0221	0.0567
(2,1)	0.0029	0.003
(1,2)	0.0038	0.0080
(2,2)	6.4356e-04	0.0010
(1,3)	8.4382e-04	0.0020
(2,3)	0.0017	0.0037
(1,4)	0.0049	0.0109
(2,4)	0.0075	0.0744

Table 4: Estimated coordinates for predefined damage locations.

Damage Cases	Case (1)				Case (2)			
	A		B		C		D	
Coordinates	x	y	x	y	x	y	x	y
Estimated	76.1	71.9	451.2	141.2	75.2	70	431.1	169.3
Actual (mm)	95	75	445	145	95	75	445	145
Accuracy %	80.1	95.8	98.6	97.4	79.2	93.3	96.9	83.2

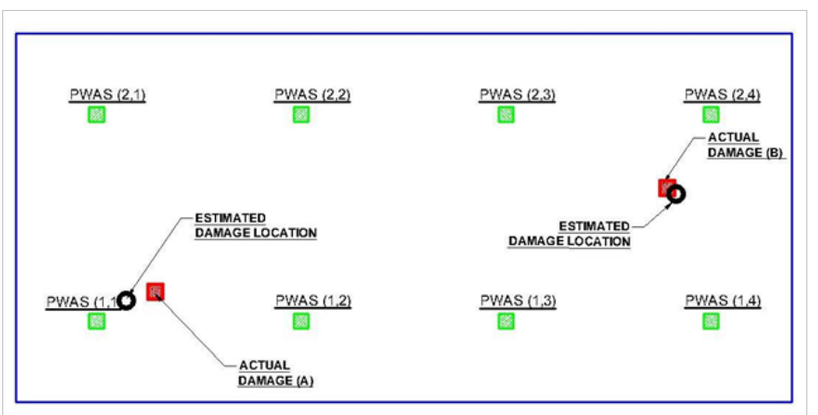

Fig. 16: Estimated damage locations for damage case (1).

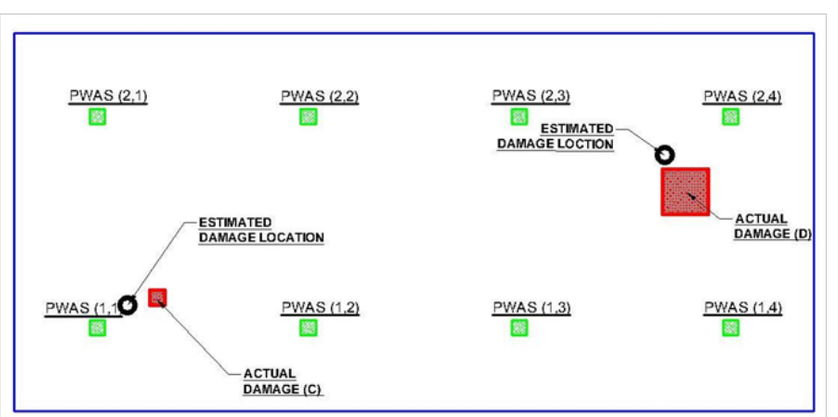

Fig. 17: Estimated damage locations for damage case (2).

IV. CONCLUSIONS

(1) The sequence of implementing the proposed algorithm subroutines makes benefit of manipulating both interrogation techniques and frequency ranges to take the advantage of each of them. This lead to handle the proposed simultaneous multi-location damage cases successfully.

(2) Figure (16) and Figure (17) show the relative accuracy of the estimated damage location for both damage cases.

(3) Applying parallel interrogation only for external PWASs, dramatically reduce the required time to detect any damage occurrence since it is simply done only for one terminal at a time instead of doing it for all PWAS individually.

(4) Applying low frequency range at elementary check, any damage existence is detected even though incipient one.

(5) Another time reduction is introduced by carry out the parallel interrogation for sub-panel to detect only the panel or panels with damage instead of going through all system.

(6) In the current study, the proposed system succeeded to estimate the location of damage with accuracy not less than 79% and up to 98% in addition to distinguish the severity of damage.

(7) Further field work is required to overcome some practical problems such as operating noise.

V. REFERENCES

[1] Cunha A., E. Caetano, and R. Delgado, "Dynamic tests on large cable-stayed bridgws.", Journal of Bridge Engineer, 2001. 6(1).
[2] Brownjohn J. and Pan T.C., "SHM of a tall building", Encyclopedia of structural health monitriong, edited by C. Boller, F. K. Chang, and Y. Funjino, 2009, John Wiley & Sons, Ltd. pp. 2233-2241.
[3] Wang X., M. Wang,Y. Zhao, H. Chen, and L. Zhou,. "Smart health monitoring system for a prestressed concrete bridge",Smart Structures and Materials Conference 2004: Sensors and Smart Structures Technologies for Civil, Mechanical, and Aerospace Systems. 2004: International Society for Optics and Photonics.
[4] Pöckl, C. and W. Kleinöder, "Developing and implementation of a fatigue monitoring system for the new European pressurized water reactor EPR",International Conference Nuclear Energy for New Europe 2007. Portoroz (Slovenia).
[5] Amin, M.S., "An integrated vibration based structural health monitoring system." Ph. D. Thesis, Department of Civil and Environmental Engineering, Carleton University Ottawa, Canada, 2002.
[6] Ewins, D.J., "Modal testing theory, practice and application." 2nd edition, Baldock, Hertordsire, England: Research Strudies Press LTD, 2000.
[7] Park, G. and C.R. Farrar, "Piezoelectric impedance methods for damage detection and sensor validation" Encyclopedia of structural health monitriong, edited by C. Boller, F. Chang, and Y. Funjino, 2009, John Wiley & Sons, Ltd. pp. 365-377.
[8] Gulizzi V., P. Rizzo, A. Milazzo, and E. Ribolla, "An integrated structural health monitoring system based on electromechanical impedance and guided ultrasonic waves". Journal of Civil Structural Health Monitoring, 2015. 5(3): pp. 337-352.
[9] De Medeiros R., D. Vandepitte, and V. Tita., "A new SHM methodology applied on composite plates." Proceedings of ISMA2016 International Conference on Noise and Vibration Engineering and USD2016 International Conference on Uncertainity in Structural Dynamics, 2016: Katholieke University Leuven, Dept. Werktuigkunde; Heverlee.
[10] Hoshyarmanesh H., A. Abbasi, P. Moein, M. Ghodsi, and K., "Design and implementation of an accurate, portable, and time-efficient impedance-based transceiver for structural health monitoring." IEEE/ASME Transactions on Mechatronics, 2017. 22(6): pp. 2809-2814.
[11] Samantaray S., S. Mittal, P. Mahapatra, and S. Kumar, "An impedance-based structural health monitoring approach for looseness identification in bolted joint structure." Journal of Civil Structural Health Monitoring, 2018. 8(5): pp. 809-822.
[12] Tzou H.S. and Tesng C.I., "Distributed piezoelectric sensor/actuator design for dynamic measurement / control of distributed parameter systems: A piezoelectric finite element approach.", Journal of Sound and Vibration, 1990. 138: pp. 17-34.
[13] IEEE Standard on Piezoelectricity, Inc, I.E.E.E.,1987: 345 East 47th Street, New York, NY 10017, USA.
[14] Ikeda, T., "Fundamentals of piezoelectricity." New York: Oxford university press, 1996.
[15] Liang C., Sun F.P., and C.A. Rogers, "Coupled electro-mechanical analysis of adaptive material systems - determination of the actuator power consumptionand system energy transfer.", Journal of Intelligent Material Systems and Structures, 1994. 5: pp. 12-20.
[16] Zagrai N.A., "Piezoelectric-wafer active sensor electro-mechanical impedance structural health monitoring" , Ph. D. in Mechanical Engineering, University of South Carolina, USA, 2002.
[17] Bhalla S., "Mechanical impedance approach for structural identification, health monitoring and non-destructive evaluation using piezo-impedance transducers.", Ph. D. in Civil and Enviromental Engineering., Nanyang technological Univeristy: Nanyang, 2004.
[18] Gresil M., Yu L., Giurgiutitu V., and Sutton M., "Predictive modeling of electromechanical impedance spectroscopy for composite materials." Journal of Structural Health Monitoring, 2012.
[19] Salem M. A., "Determination of structural integrity using advanced structural monitoring systems." M.Sc. Thesis, Civil Engineering Department., Military Technical College, Cairo, Egypt, 2017.
[20] Park G., Cudney H. H., and Inman D. J., "Feasibility of using impedance-based damage assessment for pipeline structures.", Journal of Earthquake Engineering and Structural Dynamics, 30(10): pp. 1463–1474, 2001.
[21] Hey F., S. Bhalla, and C.K. Soh, "Optimized parallel interrogation and protection of piezo-transducers in electromechanical impedance technique"., Journal of Intelligent Material Systems and Structures, 2006. 17: pp. 457-468.
[22] APC international, L.,"Physical and Piezoelectric Properties of APC Materials.", available at https://www.americanpiezo.com/apc-materials/physical-piezoelectric-properties.html, 2015.
[23] Napolitano L., F. Paolo, V. Massimo , and L. Leonardo, "Damage identification and location on a typical aeronautical structure"., SPIE 1998. 3397.
[24] Amin M. S., Abdelkhalik M., and Zidan M.K. "Structural health monitoring using two stage algorithm combines non modal-based and modal-based techniques",6th International Conference On Civil and Architecture Engineering, Military Technical College, Cairo, Egypt, 2006.
[25] Saafi M. and T. Sayyah, "Health monitoring of concrete structures strengthened with advanced composite materials using piezoelectric transducers.", Composites 2001. 32(4): pp. 333 - 342.
[26] Soh C.K., Y. Yang, and S. Bhalla, "Smart materials in structural health monitoring, control and biomechanics.", springer. 613, NewYork, 2012.
[27] Park G.H., C.R. Frrar, Rutherford A.C., and Robertson A.N., "piezoelectric active sensor self-diagnostics using elctrical impedance measurements", 15th International Conference on Adaptive Structures and Technologies, Engineering Science and Applications Weapon Response Group: Los Alamos. 2004
[28] Amin M. S. and Salem M. A., "Depolarization diagnose of PWAS used for EMI based structural health monitoring system for composite plates", 18th International Conference in Aerospace Science and Aviation Technology, Military Technical College, Cairo, Egypt, April 2019.
[29] Mechanical APDL Release 0.15, in ANSYS, Inc Products 2013., Canonsburg, Pennsylvania, USA.
[30] Salem M. A., Amin M. S. and Zidan M. K.,"Structural Health Monitoring of Composite Laminated Plates Using an Array of PWAS", 16th International Conference in Aerospace Science and Aviation Technology, May 2015, Military Technical College, Cairo, Egypt.